JACC: CARDIOVASCULAR INTERVENTIONS
VOL. 9, NO. 7, 2016

ISSN 1936-8798/$36.00
PUBLISHED BY ELSEVIER
http://dx.doi.org/10.1016/j.jcin.2015.12.018

TRANSLATIONAL

Vasomotor Function Comparative Assessment at 1 and 2 Years Following Implantation of the Absorb Everolimus-Eluting Bioresorbable Vascular Scaffold and the Xience V Everolimus-Eluting Metallic Stent in Porcine Coronary Arteries

Insights From In Vivo Angiography, Ex Vivo Assessment, and Gene Analysis at the Stented/Scaffolded Segments and the Proximal and Distal Edges

Bill D. Gogas, MD, PhD,[a,b] James J. Benham, BS,[c] Steve Hsu, PhD,[c] Alexander Sheehy, MS,[c] David J. Lefer, PhD,[d] Traci T. Goodchild, PhD,[d] David J. Polhemus, BA,[d] Yasir H. Bouchi, BS,[b] Olivia Y. Hung, MD, PhD,[a,b] Sang-Yong Yoo, MD, PhD,[a,b,e] Udit Joshi, MD,[b] Don P. Giddens, PhD,[b,f] Alessandro Veneziani, PhD,[b,g] Arshed Quyyumi, MD,[h] Richard Rapoza, PhD,[c] Spencer B. King III, MD,[a,b,i] Habib Samady, MD[a,b]

ABSTRACT

OBJECTIVES The purpose of this study was to assess and compare in vivo the restoration of vasomotor function following Absorb bioresorbable vascular scaffold (BVS) (Abbott Vascular, Santa Clara, California) and metallic Xience V (XV) (Abbott Vascular, Santa Clara, California) stent implantations in porcine coronary arteries at 1 and 2 years.

BACKGROUND Drug-eluting metallic coronary stents induce sustained vasomotor dysfunction, and preliminary observations from arteries with bioresorbable scaffolds have indicated partially restored vasoreactivity.

METHODS A total of 15 Absorb BVS (3.0 × 18.0 mm) and 14 XV (3.0 × 18.0 mm or 3.0 × 12.0 mm) stents were randomly implanted in the main coronaries of 12 nonatherosclerotic swine. The effect of implant on vasomotor performance (constrictive and expansive) was measured in the stented/scaffolded segments and the 5-mm proximal and distal adjacent segments in vivo by angiography assessing mean luminal diameter changes following infusion of vasoactive agents at 1 year (n = 6) and 2 years (n = 6) as well as ex vivo at 2 years using a tissue chamber apparatus. Endothelial cell function and smooth muscle cell phenotype gene marker levels were evaluated with quantitative real-time polymerase chain reaction.

From the [a]Andreas Gruentzig Cardiovascular Center, Division of Cardiology, Department of Medicine, Emory University School of Medicine, Atlanta, Georgia; [b]Emory Cardiovascular Imaging & Biomechanics Core Laboratory, Emory University School of Medicine, Atlanta, Georgia; [c]Abbott Vascular, Santa Clara, California; [d]Louisiana State University Health Sciences Center, New Orleans, Louisiana; [e]Gangneung Asan Hospital, Ulsan University College of Medicine, Ulsan, South Korea; [f]Wallace H. Coulter Department of Biomedical Engineering, Georgia Institute of Technology and Emory University, Atlanta, Georgia; [g]Department of Mathematics and Computer Science, Emory University, Atlanta, Georgia; [h]Emory Clinical Cardiovascular Research Institute, Department of Medicine, Division of Cardiology, Emory University School of Medicine, Atlanta, Georgia; and the [i]Saint Joseph's Heart and Vascular Institute, Atlanta, Georgia. Drs. Benham, Hsu, Sheehy, and Rapoza are employees of Abbott Vascular. All other authors have reported that they have no relationships relevant to the contents of this paper to disclose. Drs. Gogas and Benham contributed equally to this work.

Manuscript received September 21, 2015; revised manuscript received December 1, 2015, accepted December 11, 2015.

RESULTS The scaffolded Absorb BVS segments showed fully restored constrictive response compared with XV implanted vessels at 1 year: −24.30 ± 14.31% versus −1.79 ± 6.57% ($p < 0.004$) and at 2 years: −28.13 ± 14.60% versus −3.90 ± 6.44% ($p < 0.004$). The early restoration of vasomotor function within the scaffolded segments reached a peak at 1 year and did not significantly change up to 2 years. The vasoactive responses of Absorb BVS-implanted vessels within the scaffolded segments were similar to those observed within the proximal and distal edge segments at both time points. Conversely, the stented XV segments demonstrated significantly impaired constrictive response compared with the distal XV edges at 1 year: −1.79 ± 6.57% versus −21.89 ± 7.17% ($p < 0.0002$) and at 2 years: −3.90 ± 6.44% versus −21.93 ± 15.60% ($p < 0.03$). Ex vivo assessment of contraction induced by PGF2α and relaxation induced by substance P of isolated BVS segments compared with XV-treated segments generated greater contraction force of 3.94 ± 0.97 g versus 1.83 ± 1.03 g ($p < 0.05$), and endothelial-dependent relaxation reached 35.91 ± 24.74% versus 1.20 ± 3.79% ($p < 0.01$). Quantitative real-time polymerase chain reaction gene analysis at 2 years demonstrated increased Connexin 43 messenger ribonucleic acid levels of Absorb BVS-treated vessels compared with XV-treated vessels: 1.92 ± 0.23 versus 0.77 ± 12 ($p < 0.05$).

CONCLUSIONS Absorb BVS-implanted coronary arteries demonstrate early functional restoration of the scaffolded and adjacent segments at 1 year, which is preserved up to 2 years. (J Am Coll Cardiol Intv 2016;9:728–41) © 2016 by the American College of Cardiology Foundation.

Despite innovations in the field of coronary stenting, clinical restenosis and stent thrombosis rates following stent deployment in diseased coronary arterial segments remain at 5.0% and 0.4%, respectively. Furthermore, late or very late clinical events attributed to in-stent neoatherosclerosis, very late stent thrombosis, and endothelial dysfunction are being increasingly observed (1-3).

Permanent metallic drug-eluting stents (DES) with durable polymer coatings induce sustained endothelial- or nonendothelial-dependent vasomotor dysfunction after revascularization both within and distal to the implanted segments, which invariably extends during the healing phase (4,5). Endothelial dysfunction attributed to direct diffusion of the antiproliferative agent distal to treated segments or indirectly through vasa vasora remains the prevailing pathogenic mechanism. Preliminary observations from newer-generation DES have demonstrated relatively preserved endothelial-dependent vasomotor function at the proximal and distal edges compared with earlier-generation devices, whereas the in-stent segments remain dysfunctional (6).

Bioresorbable scaffolds provide a platform for vascular reparation by enabling anatomic and functional restoration during the healing phase subsequent to gradual scaffold resorption (7). Preliminary evidence derived from prospective registries, such as the ABSORB Cohorts A and B, have indicated significant anatomic and functional recovery of vessels treated with a fully resorbable scaffold during the later phases of vessel reparation (8-10).

There is a paucity of experimental comparator observations assessing short- and long-term vascular responses following deployment of permanent metallic stents and fully resorbable scaffolds in the absence of underlying atherosclerosis (11-13). Accordingly, we investigated the vasomotor and genetic responses of porcine coronary arteries treated with a permanent metallic DES, the Xience V (XV) stent (Abbott Vascular, Santa Clara, California), and a fully resorbable scaffold, the Absorb bioresorbable vascular scaffold (BVS) (Abbott Vascular, Santa Clara, California), at 1 and 2 years.

We hypothesized that Absorb BVS-treated coronary segments will demonstrate more robust functional and phenotypic recovery compared with XV-treated vessels.

METHODS

ANIMALS AND EXPERIMENTAL PROTOCOL. The study protocol was approved by the Institutional Animal Care and Use Committee and was conducted in accordance with the Association for Assessment and Accreditation of Laboratory Animal Care guidelines. Twelve healthy juvenile Yucatan mini swine (Sinclair Bio-Resources, Columbia, Missouri) underwent implantation of 15 Absorb BVS (3.0 × 18 mm) and 14 XV stents (3.0 × 18 mm and 3.0 × 12 mm) in their main coronary arteries. The lack of atherosclerosis in our model was purposely designed to investigate the differences in vasomotor function between Absorb BVS- and XV-treated vessels avoiding the

ABBREVIATIONS AND ACRONYMS

BVS = Absorb bioresorbable vascular scaffold

Cx43 = connexin 43

DES = drug-eluting stent

MLD = mean lumen diameter

QCA = quantitative coronary angiography

qPCR = quantitative real-time polymerase chain reaction

SMC = smooth muscle cell

XV = Xience V stent

confounder of underlying atherosclerosis and plaque composition, which might drive differences in endothelial response between the 2 platforms. The animals received a combination of 325 mg aspirin and 150 mg clopidogrel orally 1 day prior to implant and received 81 mg aspirin and 75 mg clopidogrel daily through the course of the 2-year follow-up. Sedation was induced by intramuscular injection of Ketamine 10 mg/kg (Vedco, St. Joseph, Missouri) and Xylazine 1 mg/kg (Lloyd Pharma, Shenandoah, Iowa), followed by intubation and general anesthesia.

SEE PAGE 742

Left heart catheterization for the in vivo assessment of restoration of treated segments was performed at 1 year (n = 6) and 2 years (n = 6) following full heparinization, achieving an activated clotting time of 250 s. Quantitative coronary angiography (QCA) was used to guide device deployment at a stent/scaffold-to-artery diameter ratio of approximately 1.1 to 1. Although this oversizing is not consistent with conventional clinical practice, it is a standard operational procedure for healthy preclinical models inducing minimal injury and avoiding device dislodgement or migration.

TREATMENT DEVICES. The Absorb BVS is a balloon-expandable scaffold consisting of a polymer backbone of poly-L-lactide coated with a thin layer of poly-D,L-lactide that forms an amorphous drug-eluting matrix containing 100 μg/cm^2 of the antiproliferative agent everolimus. A continuous decrease of the molecular weight through hydrolysis-mediated degradation as previously shown in animal models using gel permeation chromatography and echogenicity results in a gradual and steep loss of the scaffold's radial strength after 6 months. Absorb BVS is considered to be fully resorbed at between 2 and 3 years (14-18) (Online Figure A).

The XV everolimus-eluting coronary stent system is a balloon-expandable, durable polymer-coated, cobalt-chromium device. The polymer coating consists of an everolimus eluting (100 μg/cm^2) fluorinated copolymer poly (vinylidene fluoride-hexafluoropropylene). Approximately 80% of the drug is released within 30 days after implantation.

VASOMOTOR FUNCTION ASSESSMENT. An infusion catheter was passed through the guiding catheter and positioned proximal to the site of stent/scaffold implantation for the 1- and 2-year follow-up vasomotor assessment. Using a Harvard Apparatus syringe pump, incremental dose levels of acetylcholine (10^{-7}, 10^{-6}, and 10^{-5} M) were slowly administered (1.0 ml/min over 3 min), as needed, with a minimum 5-min washout period between each dose. The blood pressure and heart rate were monitored during each infusion to prevent acetylcholine-induced ischemia. The incremental dosing regimen was discontinued when the constriction was visually distinct and the subsequent dose would most likely induce an ischemic event. Angiographic images were acquired prior to and after each dose to capture the effects of acetylcholine for off-line QCA measurements. Following the effective dose of acetylcholine infusion, a bolus of nitroglycerin (300 μg) was administered to assess the vasodilatory response, and an angiogram was captured for off-line QCA analysis. Upon completion of the in vivo procedure, animals were sacrificed and the coronary arteries were harvested for tissue chamber, quantitative real-time polymerase chain reaction (qPCR) of smooth muscle cells (SMC) and functional endothelial cell markers, and histological analysis.

QUANTITATIVE CORONARY ANGIOGRAPHY. Coronary angiograms were analyzed using off-line end-diastolic QCA (QAngio XA, Medis Medical Imaging Systems, Leiden, the Netherlands) angiographic acquisitions during pre-dose, post-acetylcholine, and post-nitroglycerin infusions. Porcine coronary arteries constrict to exogenously administered acetylcholine, which in contrast to its effects in normal human coronaries, induces nonendothelial-dependent vasoconstriction acting directly on medial smooth muscle cells rather than muscarinic receptors of endothelial cells. A subsegment analysis of the artery was performed to determine the mean lumen diameter (MLD) changes of the stented/scaffolded segments and the 5-mm proximal and distal edges. Absolute MLD differences (deltas) (post-infusion - pre-infusion) were assessed as well as relative percentage MLD changes (post-infusion - pre-infusion/pre-infusion × 100%).

EX VIVO TISSUE CHAMBER APPARATUS. Isolated arterial samples implanted with Absorb BVS and XV stents were harvested and segmented for tissue chamber analysis. The arterial segments (rings) were placed on the tension apparatus within the tissue chamber (Radnoti, Glass Technology, Monrovia, California) and submersed in buffered Krebs's solution (NaCl 118 mmol/l, $MgSO_4$ 1.2 mmol/l, KH_2PO_4 1.2 mmol/l, $NaHCO_3$ 25.0 mmol/l, $CaCl_2$ 2.5 mmol/l, KCl 4.7 mmol/l, and dextrose 11.0 mmol/l at pH 7.4). The solution was enriched with 95% O_2 and 5% CO_2 at 37°C. Tension was measured using a force transducer and transmitted to a data acquisition system for

FIGURE 1 Assessment of Vasomotor Function in Absorb BVS- Versus Xience V-Treated Vessels

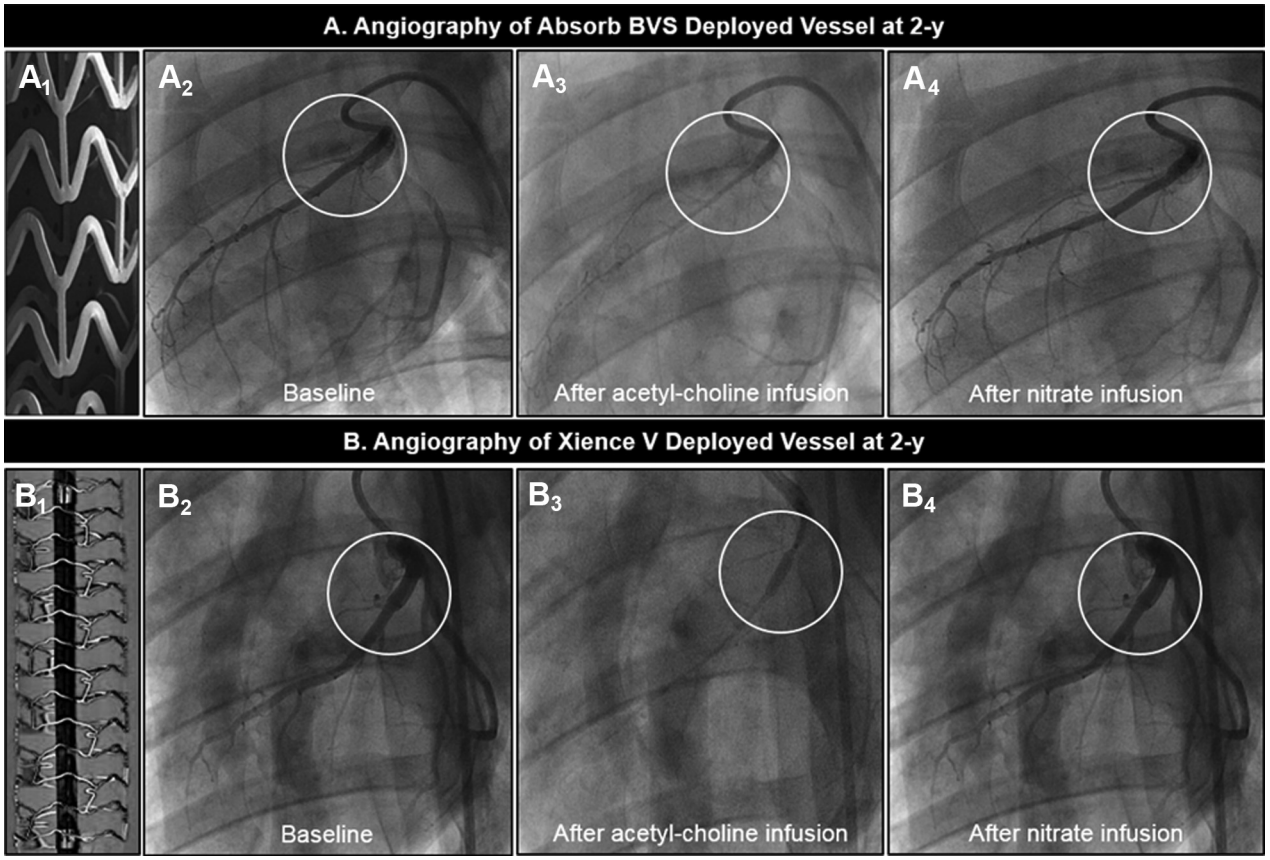

(A_1) Design of the Absorb bioresorbable vascular scaffold (BVS) everolimus-eluting scaffold. **(A_2)** Baseline angiography of the left anterior descending artery at 2 years after deployment of a fully resorbable scaffold. **(A_3)** Acetylcholine infusion induces an intense and diffuse vasospastic effect suggesting restoration of vasomotor function at this time point. **(A_4)** Nitroglycerin infusion after the vasospastic response. **(B_1)** Design of the Xience V everolimus-eluting stent. **(B_2)** Baseline angiography of the left anterior descending artery at 2 years after deployment of a metallic stent. **(B_3)** Acetylcholine infusion reveals the restriction in vasomotor performance due to the mechanic constraint induced by the metallic stent. **(B_4)** Nitroglycerin infusion after the vasospastic response.

off-line analysis. The tension was adjusted to approximately 1 g of force, and the segments were equilibrated/calibrated for a minimum of 45 min prior to the experimental challenge. Krebs's buffer solution was changed every 15 min during the equilibration period.

For each arterial ring, contracting or relaxing agents were added to assess vasomotor function. Contraction viability was assessed with 40 and 100 mmol/l KCl. Nonviable rings were discarded. Artery rings were then pre-constricted with a single dose (30 μmol/l) of prostaglandin F2-α until they reached a stable plateau. Then incremental logarithmic concentrations of substance P (0.01 to 100 pmol/l), and sodium nitroprusside (0.001 to 10 μmol/l) were used to assess the endothelial-dependent and -independent vasomotor function, respectively.

RIBONUCLEIC ACID EXTRACTION, REVERSE TRANSCRIPTION, AND qPCR. Following arterial tissue harvesting and segmenting at 1 and 2 years, untreated distal control, Absorb BVS, and XV artery tissue segments designated for gene analysis were immediately flash frozen in liquid nitrogen and stored at −80°C. Frozen tissue samples were then homogenized and isolated using TRI reagent (Ambion/Life Technologies, Grand Island, New York), and ribonucleic acid (RNA) was purified with Ribopure RNA Purification kit (Ambion/Life Technologies). Isolated RNA was treated with RNase-free DNase I to remove genomic deoxyribonucleic acid. The total RNA sample concentrations and RNA quality (A260/A280 ratio) were quantified using a Spectramax Plus spectrophotometer (Molecular Devices, Sunnyvale, California), and the quantity and quality of total RNA was further

FIGURE 2 **In Vivo Assessment of Vasomotor Function Following Implantation of the Absorb BVS and the Xience V Stent in Porcine Coronary Arteries at 2 Years**

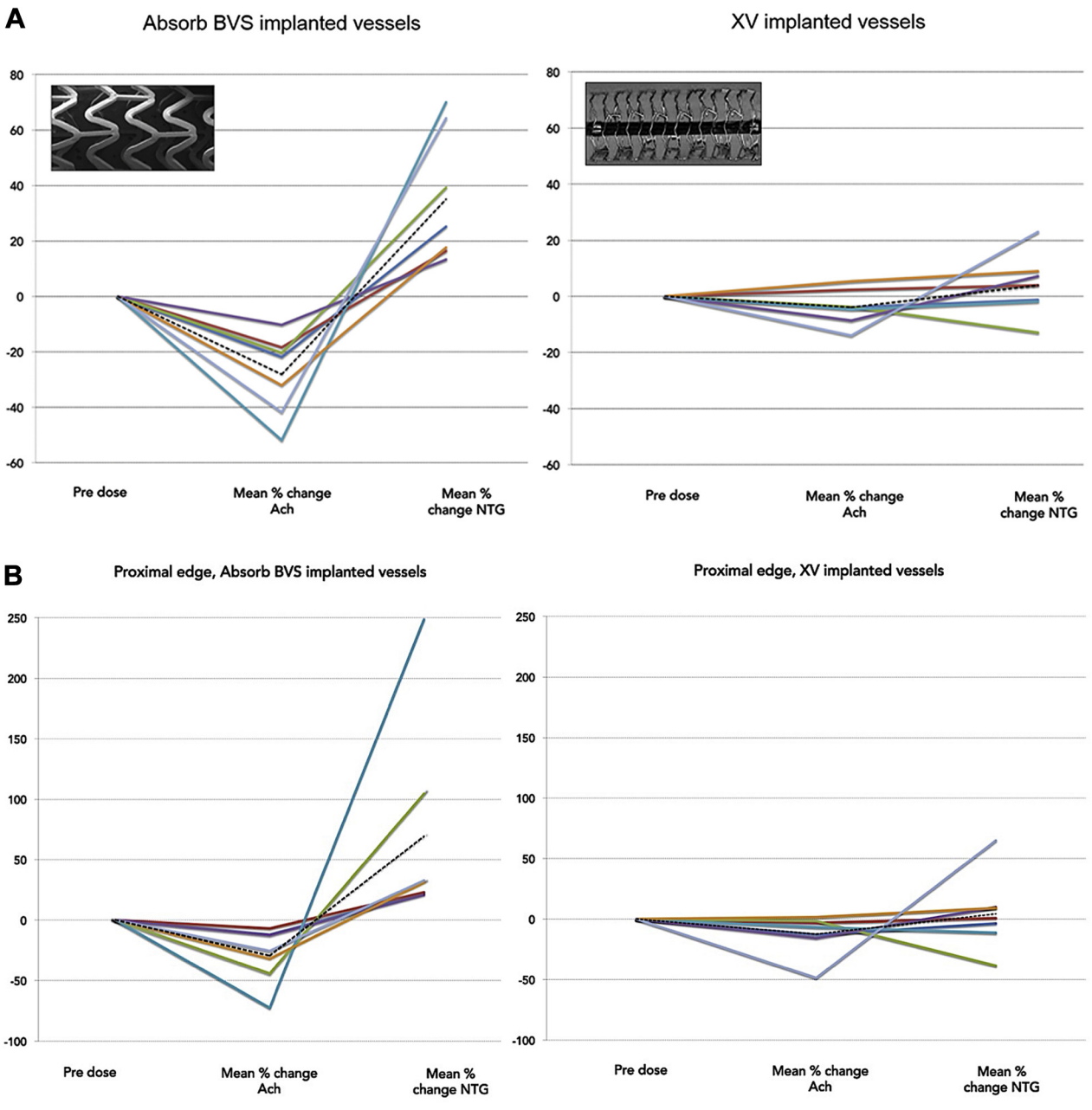

(A) In-scaffold/stent segment. **(B)** Proximal edges of Absorb bioresorbable vascular scaffold (BVS)- and Xience V (XV)-treated vessels. **(C)** Distal edges of Absorb BVS- and XV-treated vessels. Ach = acetylcholine; NTG = nitroglycerin.

Continued on the next page

validated with an Agilent Bioanalyzer (Agilent Technologies, Santa Clara, California).

Reverse transcription to synthesize first-strand complementary deoxyribonucleic acid from 10 ng RNA and Taqman qPCR were performed as previously described (19). All samples were performed in quadruplicates with the thermal cycling profile consisting of 4 stages: 50°C for 2 min, 95°C for 10 min, and 50 cycles of 15 s at 95°C and 60°C for 1 min. The threshold cycle (Ct) value of each gene was determined by the instrument's software. Relative levels of messenger ribonucleic acid (mRNA) were calculated

FIGURE 2 Continued

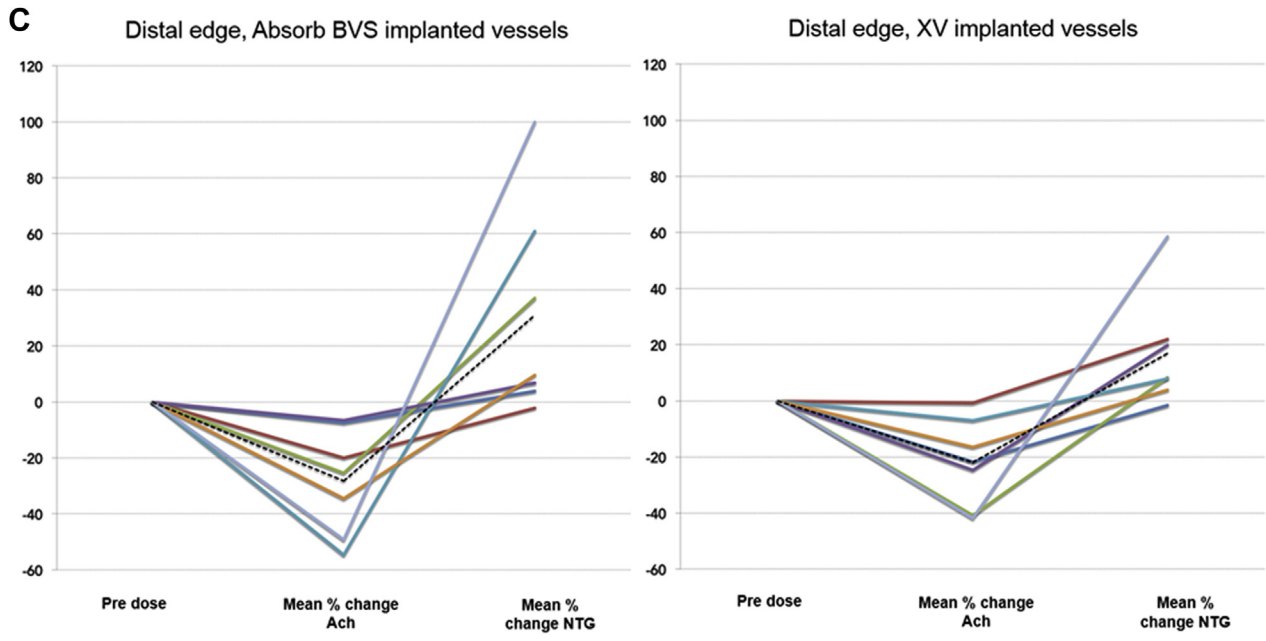

using the delta-delta Ct method, which involves comparing Ct values between samples. The relative level of target genes from the BVS and XV groups were expressed as fold change with the untreated distal control tissue as the calibrator (i.e., untreated distal control = 1) (1-year samples: control [n = 15], XV [n = 7], Absorb BVS [n = 8]; 2-year samples: control [n = 14], XV [n = 7], Absorb BVS [n = 7]).

HISTOLOGY. Absorb BVS- and XV-implanted arterial rings previously assessed in the tissue chamber at 2 years were placed in paraformaldehyde, and samples were further embedded in paraffin for histopathology and immunohistochemistry. Sections were stained with hematoxylin & eosin and Movat's pentachrome to assess the morphology.

STATISTICS. Continuous variables are reported as mean ± SD, and categorical variables as counts (%). For the in vivo and ex vivo evaluations, a Student *t* test was performed when comparing data with equal variance. Additionally, a *t* test assuming unequal variance was performed when appropriate. A p value <0.05 was considered statistically significant. A Kruskal-Wallis analysis of variance with multiple comparison Dunn's test was performed on

TABLE 1 Comparison of Percent Changes in Expansive and Constrictive Responses Following Acetylcholine and Nitroglycerin Infusions in Absorb BVS- and Xience V-Treated Vessels at 1 and 2 Years

	1 Year				2 Years			
Vasomotion Assessment	**% Change Ach**	**p Value**	**% Change NTG**	**p Value**	**% Change Ach**	**p Value**	**% Change NTG**	**p Value**
Stented/scaffolded segment								
Absorb BVS	−24.30 ± 14.31	<0.004	18.82 ± 14.97	0.12	−28.13 ± 14.60	<0.004	35.08 ± 23.51	<0.012
Xience V	−1.79 ± 6.57		7.56 ± 8.24		−3.90 ± 6.44		3.87 ± 11.12	
Proximal edge								
Absorb BVS	−21.22 ± 14.50	0.06	22.95 ± 21.27	0.37	−29.36 ± 23.09	0.15	69.10 ± 84.57	0.10
Xience V	−6.44 ± 8.22		14.96 ± 9.91		−12.51 ± 17.08		4.42 ± 31.31	
Distal edge								
Absorb BVS	−29.58 ± 13.10	0.19	25.23 ± 22.40	0.67	−28.29 ± 18.96	0.51	30.86 ± 37.80	0.41
Xience V	−21.89 ± 7.17		20.09 ± 20.15		−21.93 ± 15.60		17.01 ± 20.13	

Ach = acetylcholine; BVS = bioresorbable vascular scaffold; NTG = nitroglycerin.

TABLE 2 Comparison of Percent Changes in Expansive and Constrictive Responses in the Stented/Scaffolded Segments and the Proximal and Distal Edges of Absorb BVS- and Xience V-Treated Vessels From 1 to 2 Years

	% Change Ach			% Change NTG		
	1 Year	2 Years	p Value	1 Year	2 Years	p Value
Stented/scaffolded segment						
Absorb BVS	−24.30 ± 14.31	−28.13 ± 14.60	0.62	18.82 ± 14.97	35.08 ± 23.51	0.13
Xience V	−1.79 ± 6.57	−3.90 ± 6.44	0.98	7.56 ± 8.24	3.87 ± 11.12	0.52
Proximal edge						
Absorb BVS	−21.22 ± 14.50	−29.36 ± 23.09	0.39	22.95 ± 21.27	69.1 ± 84.57	0.21
Xience V	−6.44 ± 8.22	−12.51 ± 17.08	0.41	14.96 ± 9.91	4.42 ± 31.31	0.43
Distal edge						
Absorb BVS	−29.58 ± 13.10	−28.29 ± 18.96	0.88	25.23 ± 22.40	30.86 ± 37.80	0.73
Xience V	−21.89 ± 7.17	−21.93 ± 15.60	0.99	20.09 ± 20.15	17.01 ± 20.13	0.79

Abbreviations as in Table 1.

the qPCR data in conjunction with fold change from the control subjects to determine statistical and biological significance. A p value <0.05 and a ≥2-fold change compared with control was considered statistically and biologically significant. Analyses were conducted using SPSS package version 16.0. (SPSS Inc. Chicago, Illinois).

RESULTS

All devices were successfully deployed under angiographic guidance and all 12 animals remained healthy over the duration of the experiment.

IN VIVO ASSESSMENT. The percent constrictive change of Absorb BVS- versus XV-treated vessels following acetylcholine infusions at 1 year was: −24.30 ± 14.31% versus −1.79 ± 6.57% ($p < 0.004$) and remained significant at 2 years: −28.13 ± 14.60% versus −3.90 ± 6.44% ($p < 0.004$). The percent expansive change of Absorb BVS- versus XV-treated vessels following nitroglycerin infusions at 1 year was numerically greater in the range of 18.82 ± 14.97% versus 7.56 ± 8.24%, whereas at 2 years it reached statistical significance: 35.08 ± 23.51% versus 3.87 ± 11.12% ($p < 0.012$) (Figures 1 and 2). In-scaffold responses were of similar magnitude compared with proximal and distal edge vasomotor responses at 1 and 2 years. In particular, in-scaffold versus proximal edge percent constrictive change at 1 year was −24.30 ± 14.31% versus −21.22 ± 14.50% ($p = 0.60$), whereas at 2 years it was −28.13 ± 14.60% versus −29.36 ± 23.09% ($p = 0.91$). In-scaffold vs. distal edge percent constrictive change at 1 year was −24.30 ± 14.31% versus −29.58 ± 13.10% ($p = 0.47$) and at 2 years was −28.13 ± 14.60% versus −28.29 ± 18.96% ($p = 0.99$) (Tables 1, 2, and 3). Constrictive and expansive edge responses of XV-treated vessels at the proximal adjacent segments were dysfunctional similar to in-stent responses at 1 and 2 years. In contrast, distal edge vasoreactivity was statistically different compared with in-stent vasoreactivity.

EX VIVO ASSESSMENT IN A TISSUE CHAMBER. Contractile performance (quantified in grams) induced by PGF2-α of isolated Absorb BVS- versus

TABLE 3 Significance of the In-Segment % Changes in Constrictive and Expansive Responses at 1 and 2 Years in Absorb BVS- and Xience V-Treated Vessels

	1 Year		2 Years	
	Absorb BVS Scaffolded Segment	Xience V Stented Segment	Absorb BVS Scaffolded Segment	Xience V Stented Segment
Percent constrictive change				
Proximal edge	0.60	0.52	0.91	0.26
Distal edge	0.47	0.0002	0.99	0.03
Percent expansive change				
Proximal edge	0.68	0.37	0.26	0.96
Distal edge	0.52	0.14	0.89	0.29

All values are p values. The **top rows** indicate significance of percent constrictive changes following acetylcholine infusion in stented/scaffolded segments vs. proximal and distal edges. The **bottom rows** indicate significance of percent expansive changes following nitroglycerine infusion in stented/scaffolded segments vs. proximal and distal edges.

BVS = bioresorbable vascular scaffold.

FIGURE 3 Ex Vivo Assessment of Contraction Force (quantified as grams of force) Induced By PGF2α of Isolated Absorb BVS- and Xience V-Implanted Coronary Rings Assessed at 2 Years

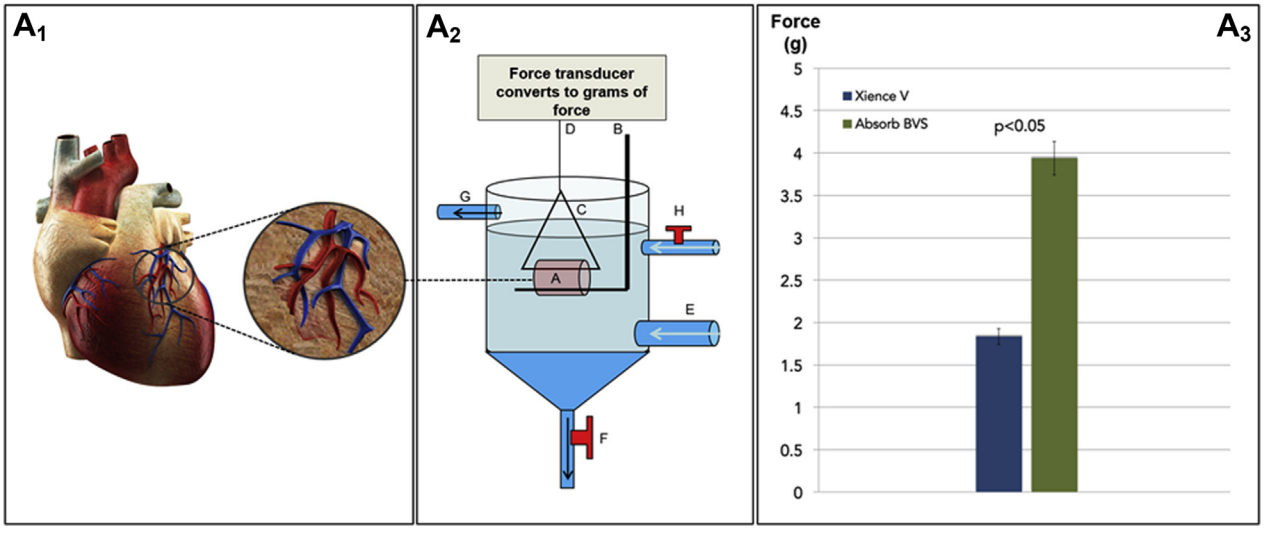

(A_1) Isolated coronary segments were harvested and segmented from the explanted hearts. **(A_2)** Segmented coronary segments placed in the tension apparatus within the tissue chamber, which consists of: **(A)** vessel segment, **(B)** lower support rod, **(C)** upper support triangle, **(D)** tension wire/thread, **(E)** oxygen supply, **(F)** drainage valve, **(G)** overflow valve, and **(H)** input valve for fresh Krebs solution. **(A_3)** Contractile performance of Absorb BVS- versus XV-implanted coronary rings induced by PGF2α.

XV-implanted coronary rings at 2 years reached 3.94 ± 0.97 g versus 1.83 ± 1.03 g ($p < 0.05$) (Figure 3). Endothelial-dependent relaxation induced by substance P reached 35.91 ± 24.74% versus 1.20 ± 3.79% ($p < 0.01$). In addition, endothelial-independent relaxation of Absorb BVS- versus XV-implanted rings assessed with logarithmic incremental infusions of sodium nitroprusside reached 82.6 ± 16.25% versus 2.99 ± 6.72% ($p < 0.05$) respectively (Figure 4).

qPCR GENE ANALYSIS. 1 and 2 years. There were no statistical and biological differences ($p < 0.05$ and ≥2-fold change) among Absorb BVS and XV groups in the mRNA levels of all functional endothelial cell markers evaluated at 1 year (Online Figure B) and 2 years (Figure 5A). The majority of SMC phenotype markers were not found to be statistically or biologically different ($p \leq 0.05$ and ≥2-fold change) between the Absorb BVS and XV groups. Only the mRNA level of Connexin 43 (Cx43) was significantly up-regulated in the Absorb BVS group compared with the XV treatment group at 2 years (Figure 5B).

Histology. Histology revealed neointima to be well organized and mild in thickness in all implants consisting of densely packed SMC organized toward the luminal surface and less dense directly surrounding struts (Figure 6).

DISCUSSION

The main findings of our study were: 1) vessel segments treated with Absorb BVS demonstrated significantly restored in-scaffold vasomotor function (constrictive and expansive) at 1 and 2 years compared with in-stent responses of XV-treated segments; 2) proximal and distal edge vasomotor responses (constrictive and expansive) adjacent to Absorb BVS-treated segments were similar to in-scaffold responses at 1 and 2 years; 3) ex vivo endothelial-dependent and -independent relaxation response of Absorb BVS coronary rings induced by substance P and sodium nitroprusside, respectively, were observed to be significantly greater as opposed to XV-treated segments at 2 years; and 4) Cx43 was significantly greater in Absorb BVS compared with XV-treated segments at 2 years.

IN VIVO ASSESSMENT. The ABSORB Cohort A (n = 30) and B (n = 101) registries assessed both endothelial-dependent and -independent vasomotor function demonstrating recovered vasomotion, which was primarily associated with the scaffold's degradation rate (20,21). To what extent functional recovery was associated with underlying plaque phenotype in these studies is unknown. This study was designed to provide mechanistic insights toward restoration of vasomotor function after Absorb BVS

FIGURE 4 Ex Vivo Assessment of Endothelial- and Nonendothelial-Dependent Vasomotor Function of Coronary Rings Assessed in a Tissue Chamber Apparatus at 2 Years

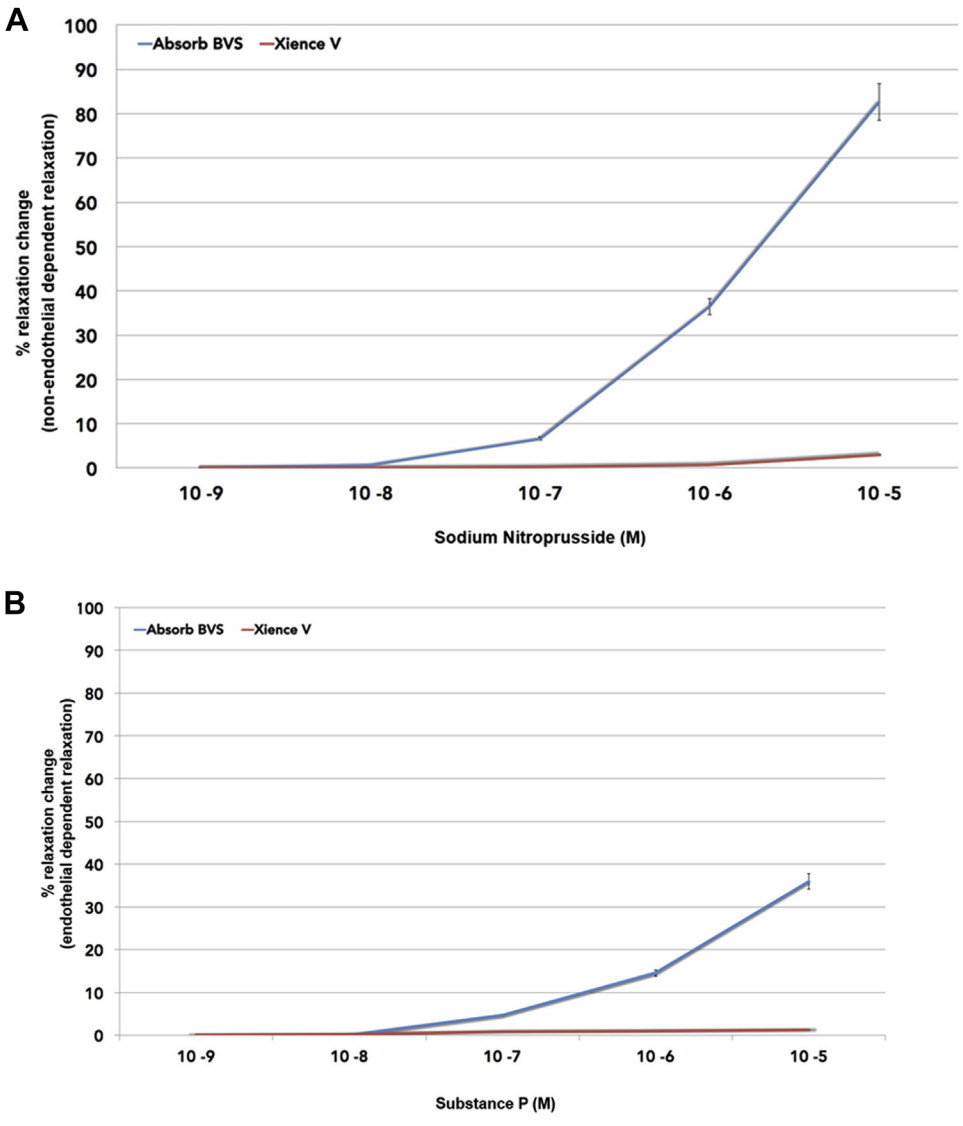

(A) Nonendothelial-dependent vasomotor function assessment with sodium nitroprusside. **(B)** Endothelial-dependent functional assessment with substance P. BVS = bioresorbable vascular scaffold.

implantation, focusing on the effect of both scaffold degradation and vascular biology eliminating endothelial dysfunction attributed to underlying atherosclerosis (8).

The reparative properties of fully resorbable scaffolds comprise the triad of initial revascularization followed by resorption and functional restoration of treated segments during the healing phase (20,22). Indeed, in this study, scaffolded vessels showed early constrictive and expansive restoration of vasomotor function at 1 year, which was preserved at 2 years, compared with the persistent and relatively mild response of XV-treated vessels (**Figure 2**).

In contrast to its effects in normal human endothelium, acetylcholine infusion induces nonendothelial-dependent vasoconstriction in healthy porcine coronary arteries acting directly on medial smooth muscle cells rather than muscarinic receptors of endothelial cells (23). In the present study, endothelial-independent vasoconstriction with acetylcholine and vasodilation with nitroglycerin showed that functional SMC-dependent vasomotion in Absorb BVS-treated

FIGURE 5 qPCR Gene Data of BVS- and XV-Treated Porcine Arterial Segments at 2 Years

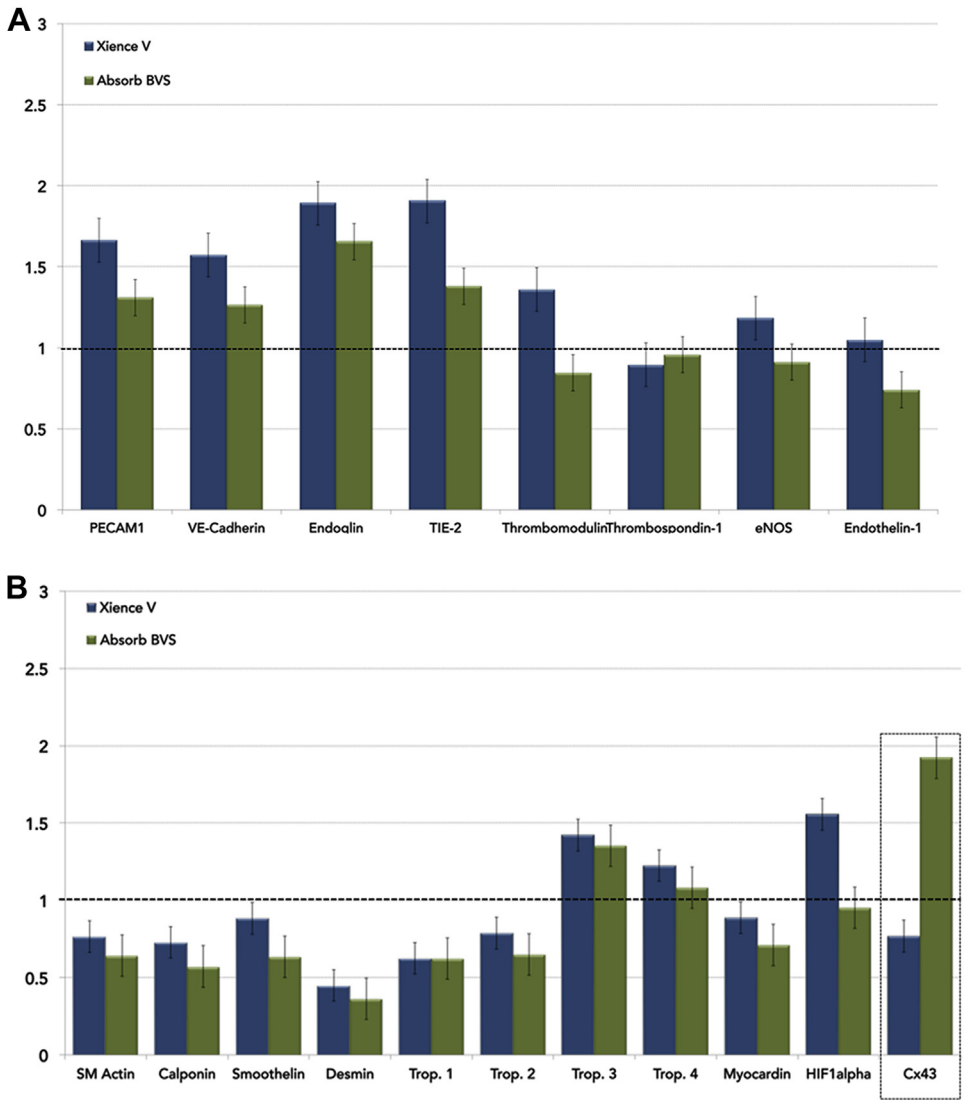

(A) Functional endothelial cell markers. **(B)** Smooth muscle cell phenotype markers. The **dashed line** indicates fold change level of control (equal to 1). BVS = bioresorbable vascular scaffold; Cx43 = connexin 43; eNOS = endothelial nitric oxide synthase; HIF1alpha = hypoxia-inducible factor-1-alpha; PECAM1 = platelet endothelial cell adhesion molecule; qPCR = quantitative real-time polymerase chain reaction; SM Actin = smooth muscle actin; Trop. = troponin; VE-Cadherin = vascular endothelial cadherin; XV = Xience V stent.

vessels are fully restored (Figure 2). This was corroborated ex vivo in a tissue-chamber apparatus by assessing contractile and relaxation responses induced by PGF2α (Figure 3) and sodium nitroprusside (Figure 4), respectively, at 2 years, indicating that an unconstrained Absorb BVS-implanted coronary segment is able to perform significantly better compared with a vessel with a permanent implant.

EX VIVO ASSESSMENT. Previous experimental studies have described similar rates of endothelial repopulation following treatment with both Absorb BVS and XV stents in porcine coronary arteries (15). Stent or scaffold deployment following coronary balloon dilation induces endothelial cell denudation. Injuries are repaired by locally derived endothelial cells or by endothelial progenitor cells, which migrate and proliferate to repopulate denuded regions (24). The integrity of endothelial-dependent vasomotor function induced by substance P was investigated in the porcine model ex vivo at 2 years. Absorb

FIGURE 6 Selected Photomicrographs of Porcine Coronary Arterial Segments at 2 Years Following Implantation of the Absorb BVS

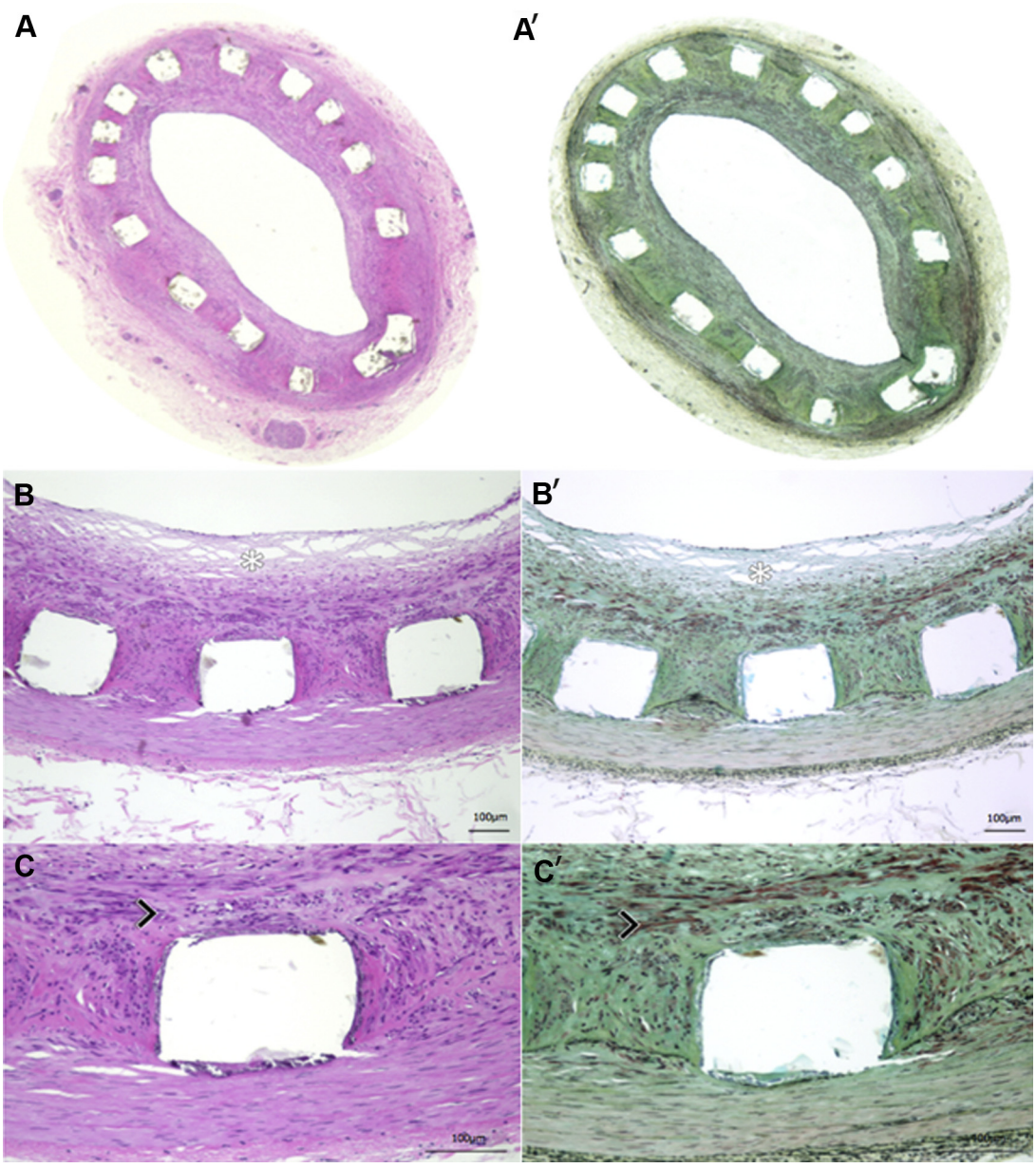

(A and A′) Struts (resorption sites) are sequestered neointima. Arteries are partially compressed due to handling for ex vivo assessment. **(B and B′)** Layering of neointimal smooth muscle cells on the adluminal aspect of struts and the subjacent media. The overlying neointimal layer shows swelling artifacts **(asterisks)** associated with tissue handling and processing. **(C and C′)** Resorption sites fully covered by neointimal tissue consisting of a layer of aligned smooth muscle cells **(arrowhead)** on collagen-rich extracellular matrix. The medial layer subjacent to struts is intact and consists of circumferentially arranged smooth muscle cells.

BVS-implanted arterial rings demonstrated significantly restored endothelial-dependent relaxation response to substance P in a dose-dependent manner compared with XV-stented rings (Figure 4), implying the presence of functional endothelium within the healed segments.

PHENOTYPIC ASSESSMENT. qPCR was used to characterize gene levels of contractile SMC phenotype markers associated with different maturity stages, and immunostaining was used to understand the relative distribution of SMC phenotypes within the arterial wall (25). Despite the observation

that vasomotor recovery occurs as early as 1 year in Absorb BVS-treated vessels, it is interesting that Absorb BVS- and XV-treated segments demonstrated no differences in SMC phenotypic expressions at 1 year (Online Figure B). By 2 years, SMC phenotypic expression of both Absorb BVS- and XV-treated vessels numerically progresses to an increasingly contractile state. This suggests that complete contractile marker expression in all SMCs of an artery is unnecessary for the artery to constrict or dilate. Instead, the loss of active scaffolding is likely the responsible component for the return of vasomotion.

The only SMC phenotypic marker that was significantly different among the treated vessels was Cx43 gene level, which was found to be up-regulated in Absorb BVS-treated compared with XV-treated tissue at 2 years. The relationship between Cx43 and SMC phenotype continues to be an area of research focus, with prior studies associating Cx43 up-regulation with 1) secretory phenotypic transition; 2) control of extracellular matrix synthesis; and 3) regulation of intimal generation following vascular injury and disease (26,27). Cx43 expression in SMCs is influenced by local mechanical forces, and it could be hypothesized that Absorb BVS, due to its thicker strut design (150 μm) compared with XV DES, applies a more diffuse mechanical footprint over the vessel wall inducing differential vascular biomechanical stress levels. These forces may activate intracellular pathways among vascular smooth muscle cells (mechanotransduction), enabling switching of SMC phenotype with changes in Cx43 expression. Increases in a single marker alone, such as Cx43, are unlikely to be sufficient to provide conclusive clinical translations; however, the up-regulation of Cx43 in Absorb BVS-treated compared with XV-treated tissue may be indicative of a continual shift toward creating a contractile "neomedia" via improved cell-to-cell communication, allowing a more coordinated modulation of vasomotor activity in the vessel wall (28) (**Figure 6**).

EDGE RESPONSE. It is also important to note that edge vasomotor dysfunction after DES implantation has been shown in both clinical and pre-clinical observations to be more prevalent at the distal rather than the proximal edge (29). The antiproliferative agent transfer via diffusion or through adjacent vasa vasora at the distal coronary conduit segments is thought to be a probable pathogenic mechanism predisposing to distal endothelial dysfunction (30). Edge vasomotor responses (constrictive and expansive) following Absorb BVS-treated vessels were restored early at 1 year and did not differ with the in-scaffold vasomotor responses either at 1 or 2 years. The aforementioned observations support the fully restored functional performance of scaffolded vessels (scaffolded segments and 5-mm proximal and distal edges).

STUDY LIMITATIONS. Although large animal models are important in vivo biomedical research tools that allow for analogous investigations with close proximity to human responses, there are numerous variations in their biological behavior that need to be taken into consideration. In regard to vasomotor reactivity, swine arterial segments respond differentially compared with human arteries (e.g., acetylcholine induces endothelial-dependent vasorelaxation in healthy human arteries as opposed to swine, which constrict, whereas assessment of endothelial-dependent relaxation in porcine arteries is evaluated with substance P).

Nondiseased porcine coronaries are state-of-the art in vivo tissues, allowing for the observation and assessment of physiological responses after exogenous stimuli excluding the interplay of diseased substrate such as atherosclerosis. Although this may appear to be a limitation of our study—as a similar assessment has already been performed in diseased human conditions—this is the novelty of the current investigation, which provides evidence of absolute physiological responses.

This observational study was not blinded to treatment assignment; however, the deployed devices in the main coronaries of healthy models as well as the same stent/scaffold size of 3.0 mm in diameter were purposely chosen to avoid any operator-dependent bias.

CONCLUSIONS

In porcine coronary arteries implanted with Absorb BVS, vasomotor function was fully restored at 1 year and remained preserved at 2 years within the scaffolded and adjacent segments as opposed to XV-stented segments.

ACKNOWLEDGMENTS The authors would like to thank Yen Chan for her technical contributions in assisting with performing qPCR assays for gene level analysis, Genus Biosystems (Northbrook, Illinois) for their assistance with RNA extraction and quantification of harvested tissue samples, and T3 Labs (Atlanta, Georgia).

REPRINT REQUESTS AND CORRESPONDENCE: Dr. Habib Samady, Emory University School of Medicine, 1364 Clifton Road NE, Suite F622, Atlanta, Georgia 30322. E-mail: hsamady@emory.edu.

PERSPECTIVES

WHAT IS KNOWN? The field of vascular reparation therapy with fully resorbable scaffolds has indicated that after the phase of acute revascularization, vessel reparation occurs.

WHAT IS NEW? This study exhibited that functional restoration and recovered endothelial-dependent vasomotor function of vessels treated with the Absorb BVS occurs early in the course of scaffold degradation.

WHAT IS NEXT? The ongoing ABSORB II randomized clinical trial, which compares the Absorb BVS to XV DES assessing a 3-year primary endpoint of vasomotor function, will address the clinical benefits of functional restoration in patients undergoing percutaneous coronary intervention.

REFERENCES

1. Gogas BD, McDaniel M, Samady H, King SB 3rd. Novel drug-eluting stents for coronary revascularization. Trends Cardiovasc Med 2014;24:305–13.

2. Farooq V, Gogas BD, Serruys PW. Restenosis: delineating the numerous causes of drug-eluting stent restenosis. Circ Cardiovasc Interv 2011;4:195–205.

3. Sarno G, Lagerqvist B, Frobert O, et al. Lower risk of stent thrombosis and restenosis with unrestricted use of 'new-generation' drug-eluting stents: a report from the nationwide Swedish Coronary Angiography and Angioplasty Registry (SCAAR). Eur Heart J 2012;33:606–13.

4. Hofma SH, van der Giessen WJ, van Dalen BM, et al. Indication of long-term endothelial dysfunction after sirolimus-eluting stent implantation. Eur Heart J 2006;27:166–70.

5. Pendyala LK, Yin X, Li J, Chen JP, Chronos N, Hou D. The first-generation drug-eluting stents and coronary endothelial dysfunction. J Am Coll Cardiol Intv 2009;2:1169–77.

6. Hamilos M, Ribichini F, Ostojic MC, et al. Coronary vasomotion one year after drug-eluting stent implantation: comparison of everolimus-eluting and paclitaxel-eluting coronary stents. J Cardiovasc Transl Res 2014;7:406–12.

7. Gogas BD. Bioresorbable scaffolds for percutaneous coronary interventions. Glob Cardiol Sci Pract 2014;2014:409–27.

8. Brugaletta S, Heo JH, Garcia-Garcia HM, et al. Endothelial-dependent vasomotion in a coronary segment treated by ABSORB everolimus-eluting bioresorbable vascular scaffold system is related to plaque composition at the time of bioresorption of the polymer: indirect finding of vascular reparative therapy? Eur Heart J 2012;33:1325–33.

9. Bourantas CV, Papafaklis MI, Kotsia A, et al. Effect of the endothelial shear stress patterns on neointimal proliferation following drug-eluting bioresorbable vascular scaffold implantation: an optical coherence tomography study. J Am Coll Cardiol Intv 2014;7:315–24.

10. Gomez-Lara J, Garcia-Garcia HM, Onuma Y, et al. A comparison of the conformability of everolimus-eluting bioresorbable vascular scaffolds to metal platform coronary stents. J Am Coll Cardiol Intv 2010;3:1190–8.

11. Puricel S, Arroyo D, Corpataux N, et al. Comparison of everolimus- and biolimus-eluting coronary stents with everolimus-eluting bioresorbable vascular scaffolds. J Am Coll Cardiol 2015;65:791–801.

12. Gogas BD, Bourantas CV, Garcia-Garcia HM, et al. The edge vascular response following implantation of the Absorb everolimus-eluting bioresorbable vascular scaffold and the XIENCE V metallic everolimus-eluting stent. First serial follow-up assessment at six months and two years: insights from the first-in-man ABSORB Cohort B and SPIRIT II trials. EuroIntervention 2013;9:709–20.

13. Farooq V, Serruys PW, Heo JH, et al. Intracoronary optical coherence tomography and histology of overlapping everolimus-eluting bioresorbable vascular scaffolds in a porcine coronary artery model: the potential implications for clinical practice. J Am Coll Cardiol Intv 2013;6:523–32.

14. Gogas BD, Farooq V, Onuma Y, Serruys PW. The ABSORB bioresorbable vascular scaffold: an evolution or revolution in interventional cardiology? Hellenic J Cardiol 2012;53:301–9.

15. Otsuka F, Pacheco E, Perkins LE, et al. Long-term safety of an everolimus-eluting bioresorbable vascular scaffold and the cobalt-chromium XIENCE V stent in a porcine coronary artery model. Circ Cardiovasc Interv 2014;7:330–42.

16. Lane JP, Perkins LE, Sheehy AJ, et al. Lumen gain and restoration of pulsatility after implantation of a bioresorbable vascular scaffold in porcine coronary arteries. J Am Coll Cardiol Intv 2014;7:688–95.

17. Campos CM, Ishibashi Y, Eggermont J, et al. Echogenicity as a surrogate for bioresorbable everolimus-eluting scaffold degradation: analysis at 1-, 3-, 6-, 12-18, 24-, 30-, 36- and 42-month follow-up in a porcine model. Int J Cardiovasc Imaging 2015;31:471–82.

18. Vorpahl M, Nakano M, Perkins LE, et al. Vascular healing and integration of a fully bioresorbable everolimus-eluting scaffold in a rabbit iliac arterial model. EuroIntervention 2014;10:833–41.

19. Hsu S, Koren E, Chan Y, et al. Effects of everolimus on macrophage-derived foam cell behavior. Cardiovasc Revasc Med 2014;15:269–77.

20. Serruys PW, Ormiston JA, Onuma Y, et al. A bioabsorbable everolimus-eluting coronary stent system (ABSORB): 2-year outcomes and results from multiple imaging methods. Lancet 2009;373:897–910.

21. Serruys PW, Onuma Y, Dudek D, et al. Evaluation of the second generation of a bioresorbable everolimus-eluting vascular scaffold for the treatment of de novo coronary artery stenosis: 12-month clinical and imaging outcomes. J Am Coll Cardiol 2011;58:1578–88.

22. Serruys PW, Onuma Y, Garcia-Garcia HM, et al. Dynamics of vessel wall changes following the implantation of the absorb everolimus-eluting bioresorbable vascular scaffold: a multi-imaging modality study at 6, 12, 24 and 36 months. EuroIntervention 2014;9:1271–84.

23. Graser T, Leisner H, Tiedt N. Absence of role of endothelium in the response of isolated porcine coronary arteries to acetylcholine. Cardiovasc Res 1986;20:299–302.

24. Kwak BR, Back M, Bochaton-Piallat ML, et al. Biomechanical factors in atherosclerosis: mechanisms and clinical implications. Eur Heart J 2014;35:3013–20, 3020a–d.

25. Rensen SS, Doevendans PA, van Eys GJ. Regulation and characteristics of vascular smooth muscle cell phenotypic diversity. Neth Heart J 2007;15:100–8.

26. Chaabane C, Otsuka F, Virmani R, Bochaton-Piallat ML. Biological responses in stented arteries. Cardiovasc Res 2013;99:353–63.

27. Cowan DB, Lye SJ, Langille BL. Regulation of vascular connexin43 gene expression by mechanical loads. Circ Res 1998;82:786–93.

28. Christ GJ, Spray DC, el-Sabban M, Moore LK, Brink PR. Gap junctions in vascular tissues. Evaluating the role of intercellular communication in the modulation of vasomotor tone. Circ Res 1996; 79:631–46.

29. Gogas BD, Garcia-Garcia HM, Onuma Y, et al. Edge vascular response after percutaneous coronary intervention: an intracoronary ultrasound and optical coherence tomography appraisal: from radioactive platforms to first- and second-generation drug-eluting stents and bioresorbable scaffolds. J Am Coll Cardiol Intv 2013; 6:211–21.

30. Gossl M, Rosol M, Malyar NM, et al. Functional anatomy and hemodynamic characteristics of vasa vasorum in the walls of porcine coronary arteries. Anat Rec A Discov Mol Cell Evol Biol 2003;272: 526–37.

KEY WORDS bioresorbable scaffolds, metal stents, porcine model, vasomotor function

APPENDIX For supplemental figures, please see the online version of this article.